Anchoring of a Ruthenium Complex in Mesoporous Silica Via a Covalent Route

Imobilização de um Complexo de Rutênio em Sílica Mesoporosa Via Rota Covalente

Ricardo D. Bernardo,[a] Pedro M. Silva Filho,[b] Maria K. S. O. Abreu,[a] Dieric S. Abreu,[b] Jackson R. Sousa,[a,†] Elisane Longhinotti,[b] Izaura C. N. Diógenes[a,*]

[a]Universidade Federal do Ceará, Departamento de Química Orgânica e Inorgânica, Laboratório de Bioinorgânica, CEP 60455-760, Fortaleza-CE, Brazil
[b]Universidade Federal do Ceará, Departamento de Química Analítica e Físico-Química, CEP 60455-760, Fortaleza-CE, Brazil

*E-mail: izaura@dqoi.ufc.br

Several approaches have been developed focusing on the irreversible attachment of compounds to solid supports aiming to avoid leaching and consequent loss of activity and recovering. Herein, we discuss the characterization of a silica-based material modified with *cis*-[RuCl(ISN)(dppb)(phen)] (RuphenISN), where ISN = isonicotinic acid, dppb = bis(diphenylphosphine)butane, phen = 1,10-phenanthroline. A stepwise strategy was adopted in which [RuCl$_2$(dppb)(phen)] was coordinated to ISN previously attached to silica through an amide coupling reaction forming the mPSi-APTS-ISN-Ruphen material. Scanning electron microscopy and N$_2$ adsorption/desorption isotherms indicated the prevalence of spherical particles of 1.5 mm. Solid ^{13}C NMR spectrum of mPSI-APTS-ISN-Ruphen showed chemical shifts in the range 170-120 ppm consistent with *sp*^{2} carbons of ISN, dppb and phen moieties. This result along with similar electrochemical response and vibrational and electronic spectral profiles of mPSi-APTS-ISN-Ruphen in respect to the non-immobilized RuphenISN complex assure the silica-based material was covalently modified. Leaching assays performed for 24 h in conditions tipycally applied in hydrogenation catalysis (basic solution at 100 ºC and 2 atm H$_2$ pressure) showed no complex in solution meaning the silica-based material covalently modified with RuphenISN is robust enough to keep the compound into the silica, ensuring its recycling and reuse if applied in such processes.

Keywords: Mesoporous silica; ruthenium complex; coordination chemistry; covalent anchoring.

1. Introduction

The easiness of tuning structural properties by simple altering the reaction conditions has been claimed as one of the major advantages of porous materials when envisioning specific applications because of the possibility of rationally control the physicochemical features.[1-3] Among porous materials, silica-based ones have caught the attention due to the easiness of attaching functional groups at either the external and internal surface porous.[2-4] This versatility has allowed the use of silica-based materials as adsorbents,[3] biomolecules immobilization,[5,6] gas storage,[7] sensors,[8] drug release,[2,5,9] and support for catalysts.[10-12] In heterogeneous catalysis, it is crucial to have catalyst supports that provide mechanical resistance, high surface area, and thermal stability. Besides these features, silica-based supports are insoluble in almost all organic solvents facilitating the removal from the reaction mixture. Several works have been published focusing on the functionalization of silica aiming to use it as support structure for catalysts in many processes including catalytic hydrogenation of aromatic hydrocarbons.[11-13] The catalytic hydrogenation of acetophenone to 1-phenylethanol, a relevant reaction in fine chemical industries, is usually performed by using palladium or rhodium in homogeneous media implying high costs due to the need of purification because of both the presence of the catalyst and undesirable side-products.[4,11] Coordination compounds of ruthenium(II), which is far less expensive than palladium or rhodium, bearing arenes and/or phosphine-based ligands have emerging as a low-cost and efficient alternative for the catalysis of hydrogenation reactions of ketones.[4,12,14-17] In a step further, aiming to join efficiency with cost reduction, coordination compounds containing ruthenium(II), have been attached to silica-based supports for applying as heterogeneous catalysts.[4,10,13,18,19] In this context, ruthenium complexes containing bipyridine derivatives were anchored on silica nanoparticles for catalytic hydrogenation of ketones and oxidation of thioanisole and alcohols giving conversion efficiencies higher than 70%.[20,21]

Despite the advantages of the silica-based supports of being unexpensive and easily removed from liquid media, the catalyst must be strongly attached to the support to avoid leaching with consequent loss of catalytic activity and recovering. Indeed, the growing awareness

of chemical industries on environmental issues requires recycling and reuse of the catalyst after the reaction. A wide range of strategies, covalent and non-covalent, has been developed aiming efficient procedures to attach catalysts to solid materials wherein the covalent ones have given the best results.[9,19,22,23] However, because the attachment of complexes in solid confined spaces is not an easy task, just a few reports can be found regarding the modification of silica-based materials with ruthenium compounds.[4,9,10,13,18-22,24]

Knowing that complexes of the type [RuCl(dppb)(L1)(L2)], where dppb = 1,4-bis(diphenylphosphine)butane, and L1 and L2 are pyridine and phenanthroline derivatives, have shown high catalytic efficiencies in reactions of ketone hydrogenation,[15,17,25,26] the main goal of this work is to present an approach for the modification of mesoporous silica (mPSi) through the direct coordination of a ruthenium metal center to isonicotinic acid (ISN) previously attached to mPSi. By doing that, we intend to assure that there will be no leaching of the complex from the solid support thus allowing recycling and reuse if applied in heterogeneous catalysis. Textural, morphological, spectroscopic, and electrochemical studies will provide evidence of the modification of the silica-based material with *cis*-[RuCl(ISN)(dppb)(phen)] (mPSi-APTS-ISN-Ruphen), where phen = 1,10-phenanthroline.

2. Experimental

2.1. Chemicals

Tetraethylorthosilicate (TEOS, Aldrich, 99%), chitosan (degree of deacetylation: 86%; MM: 480000g/mol), aerosil® fumed silica, 3-aminopropyltriethoxysilane (APTS, Aldrich, 98%), N,N'-diisopropylcarbodiimide (DIC, Sigma-Aldrich, 99%), dimethylformamide (DMF, Merck, 99%), toluene (Merk, 99%), ethanol (Merck, 99%), isopropyl alcohol (Tedia, 99.9%), isonicotinic acid (ISN, Sigma-Aldrich, 99%), ruthenium trichloride (Sigma-Aldrich, 99.98%), 1,4-bis(diphenylphosphine)butane (dppb, Sigma-Aldrich, 98%), 1,10-phenanthroline (phen, Sigma-Aldrich, 99%), dichloromethane (Tedia 99.8%), trifluoroacetic acid (Tedia, > 99%), KOH (Synth, 85%), and NaOH (Synth, 97%) were used without further purification.

2.2. Synthesis of the precursor complexes {[RuCl$_2$(dppb)]$_2$-μ-(dppb)} and *cis*-[RuCl$_2$(dppb)(phen)]

{[RuCl$_2$(dppb)]$_2$-μ-(dppb)} was synthesized according to the literature procedure.[27] C*is*-[RuCl$_2$(dppb)(phen)] was synthesized following the procedure described in the literature[28] with minor modifications. In brief: 220.0 mg (0.12 mmol) of {[RuCl$_2$(dppb)]$_2$-μ-(dppb)} and 21.6 mg (0.12 mmol) of 1,10-phenanthroline (phen) were dissolved in 25 mL of previously deaerated toluene and the mixture

was left under stirring for 48 h followed by hexane addition to force precipitation. The obtained solid was washed with hot hexane and dried under vacuum. Yield: 90%.

2.3. Synthesis of *cis*-[RuCl(dppb)(ISN)(phen)](PF$_6$)

The compound *cis*-[RuCl(dppb)(ISN)(phen)](PF$_6$) was synthesized in homogeneous medium to provide evidence for the characterization of the silica material modified with this complex *via* a covalent route which will be further detailed. For the homogeneous synthesis, we adopted a protocol similar to that reported by Smith *et al.*[29] A mixture containing 100 mg (12.8 mmol) of *cis*-[RuCl$_2$(dppb)(phen)] and 15.6 mg (12.8 mmol) of isonicotinic acid in 20 mL of dried ethanol was left under reflux for 72 h in dark. After that, the orange solution was filtered and had the volume decreased to 5 mL through rotary evaporator. Precipitation was observed after the addition of a saturated aqueous solution of NH$_4$PF$_6$. For purification, the obtained solid was applied to a Sephadex column. Yield: 65%. anal. ^{1}H NMR (500 MHz, CDCl$_3$, Figure S1) δ in ppm: 1.74 (2H of CH$_2$), 2.4-3.0 (6H of 3CH$_2$), 4.5 (NH), 6.9-8.1 (32H, 20H of PPH$_2$, 8H of phen, and 4H of ISN). ^{13}C NMR (500 MHz, CDCl$_3$, Figure S2) δ in ppm: 128 (C3 and C5 of dppb; C2 and C4 of ISN; C4 and C5 of phen), 129 (C2 and C7 of phen), 130 (C4 of dppb), 131 (C2 and C6 of dppb; C3 and C6 of phen).

2.4. Synthesis of porous silica microspheres (mPSi)

Porous silica microspheres were prepared according to previous reported procedure[30] with minor modifications. 50 mg of aerosil® silica, 3 mL of TEOS, and 8 mL of ethanol were added to a chitosan emulsion (0.3 g of chitosan in 10 mL of a 2.5% v/v aqueous solution of acetic acid). After 4 h of stirring, a 15% v/v ammonium hydroxide solution was dropwise added forming silica microspheres (mPSi). The microspheres were dried for 48 h at room temperature and calcined for 2 h at 550 °C with a heating rate of 5 °C/min in air flow.

2.5. Immobilization of *cis*-[RuCl$_2$(dppb)(phen)] into mPSi

Silica microspheres were functionalized with 3-aminopropyltriethoxysilane (APTS) according to the literature[31,32] as follows: 1.0 g of mPSi activated at 110 °C under vacuum for 4 h were transferred to a reactional flask containing 0.8 mL of APTS dispersed in toluene. The mixture was kept under reflux and argon for 48 h when the solid was filtered, washed with toluene and ethanol, and dried under vacuum. The functionalized material (1.0 g) was added to another reactional flask containing 7.08 mmol of isonicotinic acid (ISN) and 1.77 mmol of N,N'-diisopropylcarbodiimide (DIC) dissolved in DMF. The mixture was kept under stirring for 24 h at 60 °C and the solid, named mPSi-APTS-ISN, was filtered, washed with DMF and ethanol and dried under vacuum. This material

(0.10 g) was added to a Schlenk flask containing 25 mL of a 6.42 x 10^{-2} mmol L^{-1} solution of *cis*-[RuCl$_2$(dppb)(phen)] in dichloromethane and kept under argon, reflux and stirring for 48 h. After that, the non-immobilized complexes were removed with dichloromethane in a Soxhlet apparatus for 48 h. The modified microspheres were dried for 2 h at 60 °C and stored under vacuum.

2.6. Leaching assays

For the leaching assays, 40 mg of mPSI-APTS-ISN-Ruphen were added to a Schlenk flask containing 9.5 mL of isopropyl alcohol and 0.5 mL of a 0.02 mol L^{-1} solution of KOH in isopropyl alcohol. The mixture was kept under stirring for 24 h at 100 °C and 2 atm H_2 pressure to mimic the conditions typically applied in catalytic hydrogenation reactions of ketones. The amount of complex leached into the solution was verified by electronic spectroscopy in the ultraviolet and visible (UV-Vis) regions.

2.7. Apparatus

Elemental analyses were performed in a Perkin Elmer model 2400 series II analyzer. The experiments were run in triplicate using 20 mg of sample. The morphology of the nanoparticles was investigated by Scanning Electron Microscopy (SEM) using a FEG Quanta 450 electron microscope equipped with energy dispersive spectroscopy (EDS) Bruker QUANTAX system (20 kV). Textural properties were studied by N_2 adsorption-desorption isotherms and measured on a Quantachrome Autosorb−1B instrument at the temperature of liquid nitrogen. All samples were degassed at 250 °C prior to the measurements. The specific surface area of the samples was calculated using the BET method.[33] The pore size distribution was derived from the adsorption branches of the isotherms using the Barrett–Joyner–Halenda (BJH) method.[34] Solid-state ^{13}C and ^{29}Si cross polarization/magic angle spinning (CP/MAS) nuclear magnetic resonance (NMR) spectra were recorded on a Bruker Avance II+400 NMR spectrometer operating at 100.6 and 79.49 MHz, respectively. The ^{13}C NMR spectra were obtained with contact time of 3 ms and the chemical shifts are reported relative to adamantane. The ^{29}Si NMR spectra were recorded with high power decoupling (HPDEC) with a repetition time of 60 s and an angle of 90°. Kaolinite was used as a reference standard. For the ^{1}H and ^{13}C NMR spectra in CDCl$_3$ solution, it was used an AVANCE DPX 500 Bruker spectrometer operating at 500 MHz. Electronic absorption spectra in the UV-Vis regions were acquired in a Varian spectrophotometer model CARY 500. The samples were prepared as thin films typically containing 2 mg of the sample in 55 mg of KBr. Infrared spectrophotometer (FTIR/ABB; FTLA 2000) was used in the range of 4000 to 400 cm^{-1} and the samples were prepared as KBr pellets containing 1% wt%. Electrochemical measurements (cyclic voltammetry) were performed using

an electrochemical system from Bioanalytical Systems, model BAS Epsilon. The experiments were carried out at 25 °C using a conventional three-electrode glass cell with platinum wire and Ag/AgCl (3.5 mol L^{-1} KCl, BAS Inc.) as auxiliary and reference electrodes, respectively. As working electrode, it was used a carbon paste prepared by mixing 40.0% of mPSI-APTS-ISN-Ruphen in activated carbon suspended in mineral oil (Nujol®). The NaTFA electrolyte solution (pH 3.50) was prepared by dilution of the concentrated trifluoracetic acid (HTFA) to 0.1 mol L^{-1} followed by pH adjusting to 3.50 by the addition of NaOH. The thermogravimetry and differential thermal analysis (TG-DTA) curves were obtained using a thermal analysis system (Shimadzu, DTA-60H model). The samples were heated from 25 to 1000 °C using open alumina crucibles with approximately 10 mg of the sample under an oxygen atmosphere, at a heating rate of 10 °C min^{-1}.

3. Results and Discussion

Prior to the immobilization of *cis*-[RuCl$_2$(dppb)(phen)] into the silica microspheres (mPSi), the material was functionalized with 3-aminopropyltriethoxysilane (APTS) and bonded to isonicotinic acid (ISN) as detailed in the Experimental Section and schematically illustrated in Figure 1.

The characterization of the material will be presented starting with the elemental analysis of the silica-based samples, shown in Table 1.

As expected, the percentage of C and N increase on going from the non-modified mPSi material to mPSI-APTS-ISN-Ruphen indicating the attachment of the APTS, ISN, and Ruphen moieties. Such conclusion will be reinforced in the following discussions.

After the determination of the values of %C, %N, and %H, the micrographs and textural analyses of the silica-based samples will be presented followed by the NMR data, vibrational, electronic, electrochemical, and thermogravimetric results intending to prove the silica-based material was covalently modified with [RuCl(dppb)(ISN)(phen)]$^+$ producing the mPSI-APTS-ISN-Ruphen material. Aiming to support the characterization of mPSI-APTS-ISN-Ruphen, the *cis*-[RuCl(dppb)(ISN)(phen)](PF$_6$) complex was synthesized in homogeneous medium and fully characterized.

3.1. SEM analyses and textural features

The morphological and textural properties were evaluated by means of scanning electron microscopy (SEM) and N_2 adsorption/desorption analyses. Figure 2 shows the SEM images obtained for the silica-based material where it can be seen spherical and rod-shaped particles of average size of 1.5 mm, with the former geometry prevailing. The material, therefore, can be classified as rough microspheres
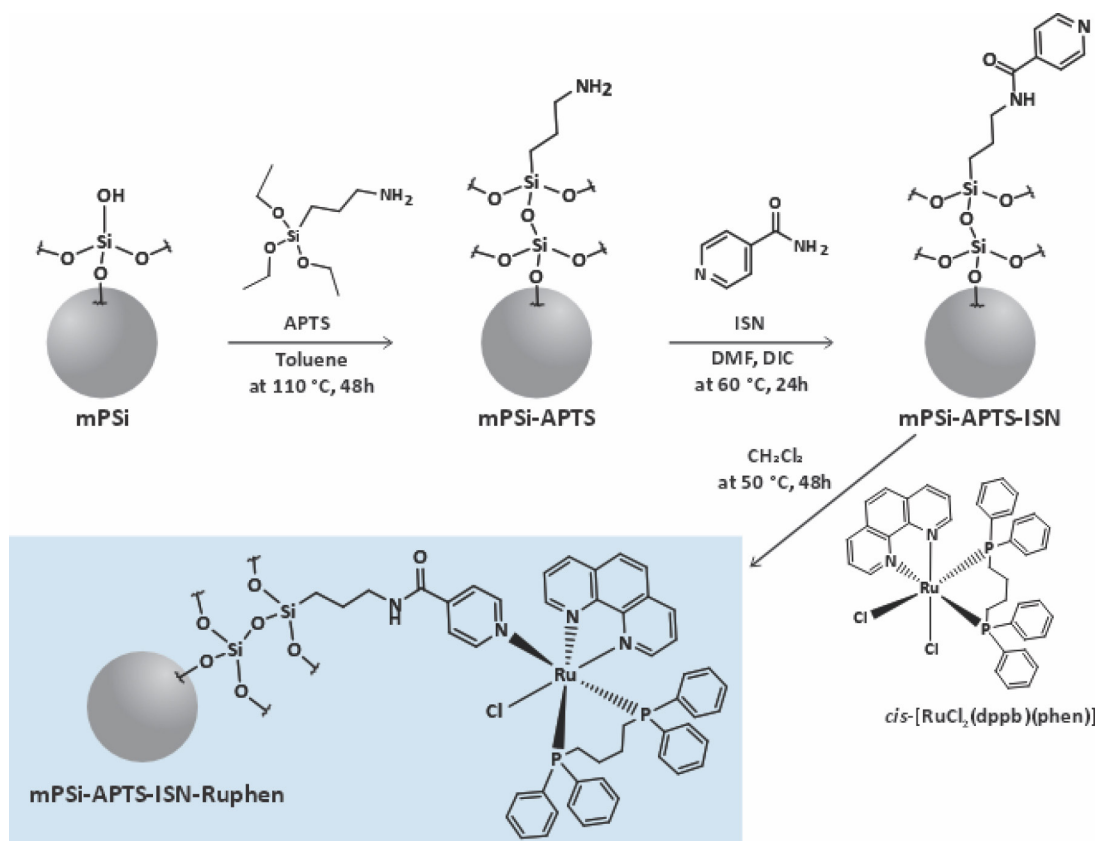
Figure 1. Cartoon illustration of the synthetic steps for the immobilization of *cis*-[RuCl$_2$(dppb)(phen)] on silica microspheres (mPSi) producing mPSi-APTS-ISN-Ruphen

Table 1. Values of %C, %N, and %H (average of triplicate measurements) determined for the non-modified silica (mPSi), and modified with APTS (mPSI-APTS), APTS and ISN (mPSI-APTS-ISN), and APTS, ISN and [RuCl(dppb)(phen)]$^+$ (mPSI-APTS-ISN-Ruphen)

Sample	%C	%N	%H
mPSi	1.89	0.59	1.06
mPSI-APTS	7.13	2.90	2.15
mPSI-APTS-ISN	7.22	2.78	1.89
mPSI-APTS-ISN-Ruphen	10.3	3.04	1.93

containing a few cracks on surface. Similar micrographs were obtained at all modification steps meaning the molecules added during the stepwise procedure do not alter the morphological features of the silica-based material.

The existence of porous as suggested by the rough aspect of the material was analyzed by N$_2$ adsorption/desorption isotherms which are illustrated in Figure 3.

The obtained isotherms (Figure 3A) are similar for the adsorption and desorption processes for each sample and present a H4 hysteresis loop and profiles consistent with a type IV according to the IUPAC classification.[35] The observation of the H4 hysteresis loop suggests the material is composed by two types of pores, *i.e.* micro and meso porous.[36,37] Indeed, the pore size distribution evaluated by BJH method,[34] indicates the majority of the porous are within the microporous region (< 2 nm) with significant contribution in the mesoporous range (2 to 50 nm). The

values of surface area, pore diameter, and pore volume are summarized in Table 2.

The successive modifications of mPSi with APTS and the ruthenium complex resulted in a decrease of the surface area, pore diameter, and pore volume. Except for the pore diameter parameter that shows an opposite trend, the observed decrease of the surface area and pore volume is expected due to the filling of the free spaces. For the mPSi-APTS-ISN-Ruphen sample, however, a meaningful increase of the pore diameter is observed in respect to mPSi-APTS. This result is very likely associated to a disruption of the outermost pores that leads to a diameter increase. Such suggestion is reinforced by the SEM micrographs obtained for mPSi-APTS-ISN-Ruphen (Figures 3 C and D) in which it can be seen pores of 56 μm of diameter. This porosity, in turn, may imply advantage for the mPSi-APTS-ISN-Ruphen material to be used in
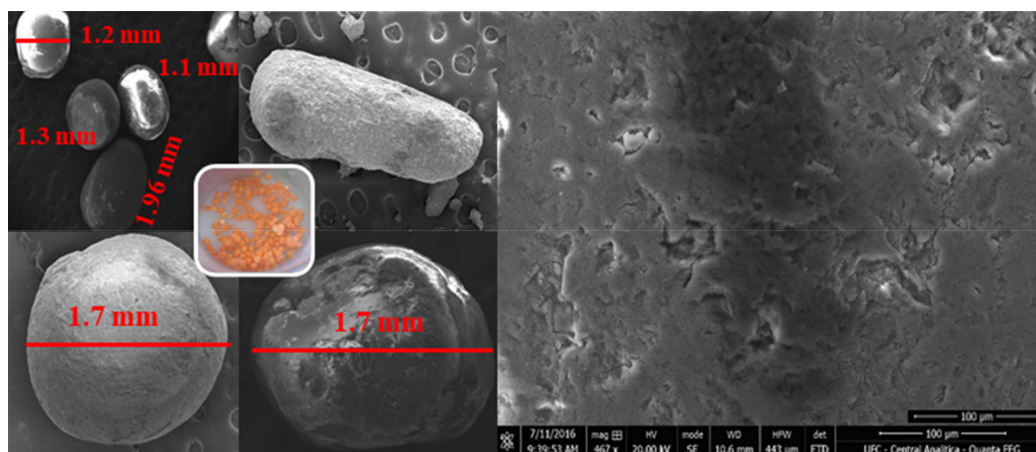
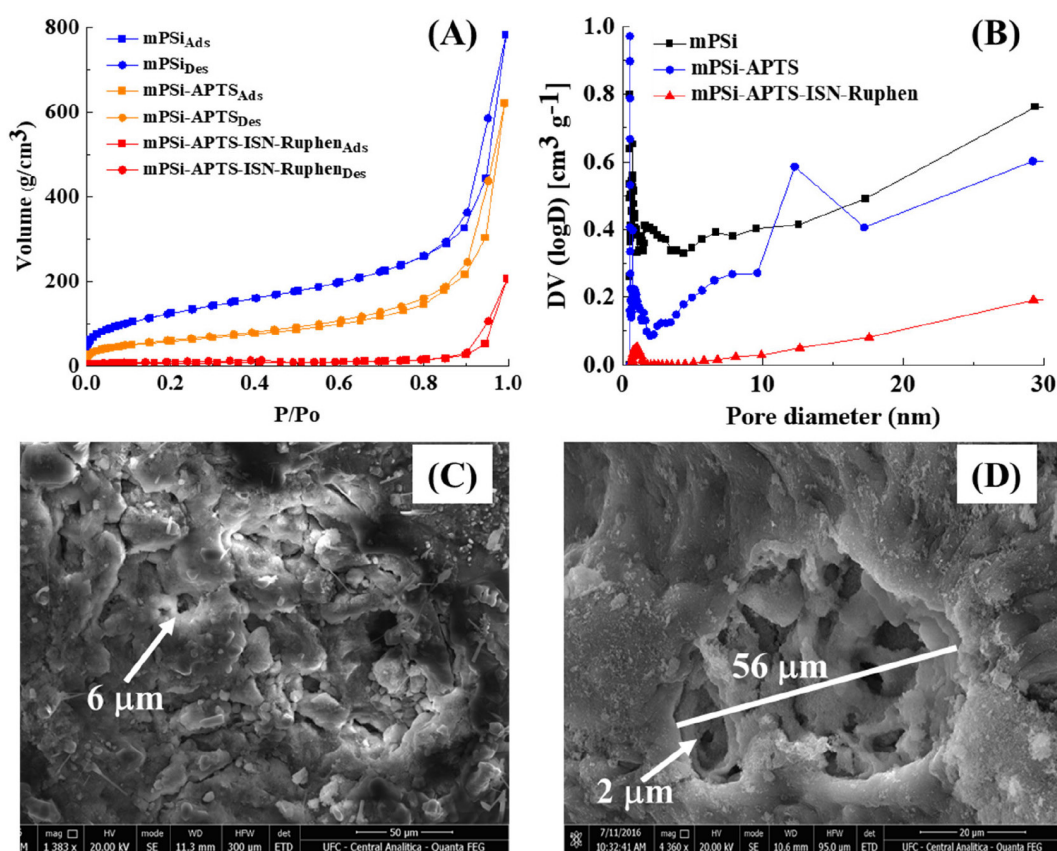**Figure 2**. Scanning electron microscopy (SEM) image of mPSi

Figure 3. (A) N_2 adsorption/desorption isotherms and (B) pore size distributions obtained for mPSi, mPSI-APTS, and mPSI-APTS-ISN-Ruphen. The subscripts Ads and Des stand for adsorption and desorption, respectively. SEM micrographs of mPSI-APTS-ISN-Ruphen in scales of 50 µm (C) and 20 µm (D)

Table 2. Surface area (S_{BET} m²/g), pore diameter (nm), and pore volume (cm³/g) of the silica-based samples as determined by N_2 adsorption/desorption isotherms.

Sample	Surface area (S_{BET} m²/g)	Pore diameter (nm)	Pore volume (cm³/g)
mPSi	1515	0.70	1.412
mPSi-APTS	735.5	0.50	1.059
mPSi-APTS-ISN-Ruphen	21.54	0.80	0.3296

Acronymous. mPSi: non-modified silica; mPSI-APTS: silica modified with 3-aminopropyltriethoxysilane (APTS); mPSI-APTS-ISN-Ruphen: silica modified with APTS and isonicotinic acid (ISN) covalently bonded to [RuCl(dppb)(phen)].

heterogeneous catalysis where large surface areas are desired. Also, porous materials facilitate the substrate diffusion into the pores thus improving the activity and selectivity of the catalyst.[38]

3.2. ^{29}Si and ^{13}C CPMAS NMR spectrometry

Figure 4 shows the ^{29}Si CP-MAS NMR spectra in the solid state obtained for the silica-based microspheres before and after the functionalization with APTS.

Chemical shifts observed at -109 (Q^4) and -100 ppm (Q^3) are assigned[39] to $(Si-O)_4Si$ and $(Si-O)_3SiOH$ groups. The shifts observed at -57 and -67 ppm, marked as T^2 and T^3, respectively, in the spectrum of mPSi-APTS (solid blue line), are associated[40] with the $(Si-O)_2SiROH$ and $(Si-O)_3SiR$

groups, where R = $CH_2CH_2CH_2NH_2$. The observation of these chemical shifts proves the occurrence of the condensation reaction resulting in the functionalization of the silica-based material with APTS.

The ^{13}C CPMAS NMR spectra obtained for mPSi-APTS, mPSi-APTS-ISN, and mPSI-APTS-ISN-Ruphen are shown in Figure 5. For the mPSi-APTS sample, chemical shifts typical of sp^3 carbons are seen at *ca* 40, 20, and 10 ppm being assigned[40] to C3($\bullet$), C2($\bullet$), and C1($\bullet$) carbons, respectively, thus reinforcing the indication of the functionalization with APTS.

The spectrum of mPSi-APTS-ISN presents additional chemical shifts within the region 120-180 ppm with that at 165 ppm ($\bullet$) being assigned[24] to the carbon of the amide group, whereas those at 120, 140, and 150 ppm are ascribed[41]
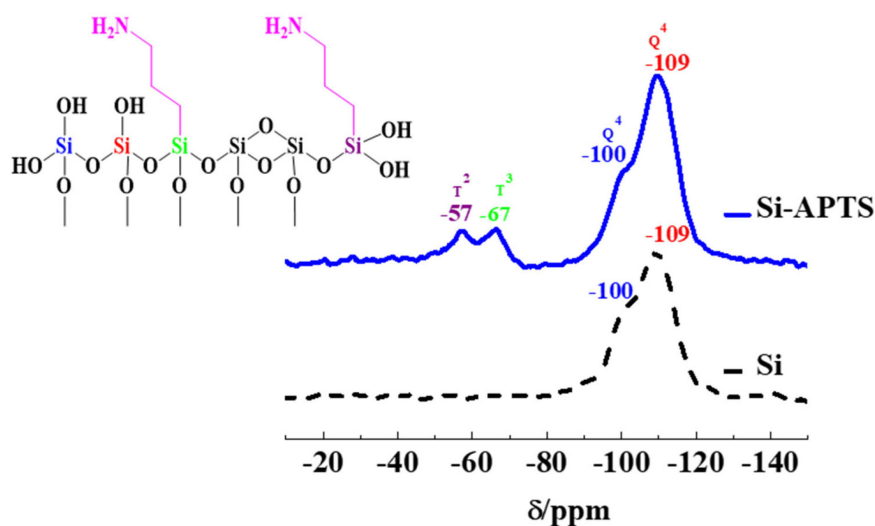
Figure 4. ^{29}Si CP-MAS NMR spectra in the solid state obtained for the mPSi (blue solid line) and mPSi-APTS (dotted black line) samples along with an illustration of a silica chain with silicon atoms bonded to four oxygen atoms in a tetrahedron symmetry highlighting the attachment of APTS (in magenta)

Figure 5. ^{13}C NMR spectra obtained for mPSi-APTS (a), mPSi-APTS-ISN (b), and mPSI-APTS-ISN-Ruphen (c). Filled colored circles are used for matching the chemical shifts with the structures displayed at the left side of the figure

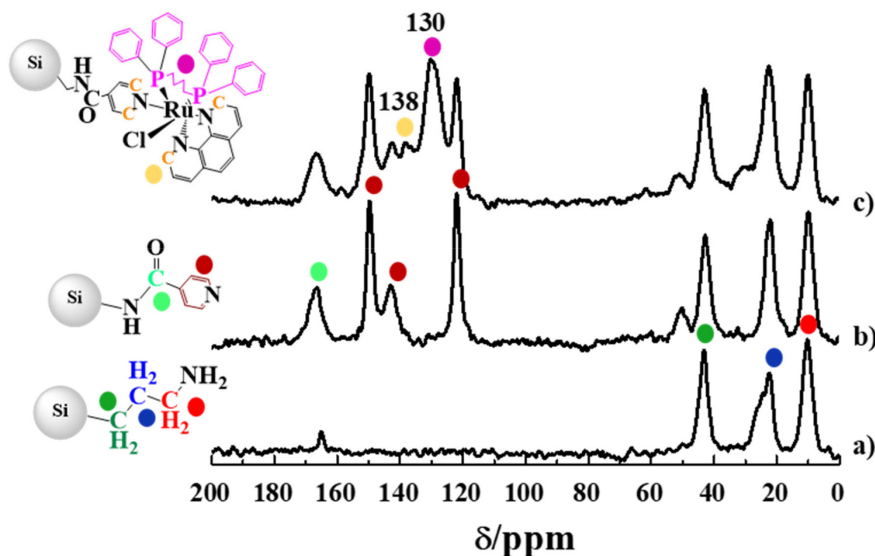to the sp^2 carbon of the ISN ligand. For the mPSI-APTS-ISN-Ruphen sample, the spectrum (Figure 5, c) shows the emergence of new chemical shifts from 120 to 140 ppm indicating an increase of the sp^2 carbons which is consistent with the presence of the phen and dppb molecules. Indeed, the shifts observed at 130 and 138 ppm are assigned,[42] respectively, to the dppb (●) and phen (○) fragments of the ruthenium complex confirming the immobilization of this species on the silica-based material.

3.3. Vibrational and electronic analyses

Silica-based materials functionalized with APTS give typical vibrational profiles that make infrared (IR) spectroscopy a fundamental tool for characterizing them. Figure 6 (A) shows the IR spectra acquired at each step of preparation. For the non-modified silica, the stretching modes of the siloxane groups, ν(Si-O-Si), are seen at around 1080 cm^{-1}, whereas the angular deformation (δ) is observed at 470 cm^{-1}.[43] The strong absorption of the stretching modes of the siloxane groups dominates the IR spectra in all steps of the material modification.

The bands observed from 2921 to 2877 cm^{-1}, assigned[43] to the vibrational modes of the CH and CH$_2$ bonds of APTS, indicate this compound was immobilized on mPSi. Also, the stretching mode assigned[43] to the C-Si bond is observed discreetly at 700 cm^{-1} in the spectrum of mPSi-APTS reinforcing this conclusion. After the amide coupling mediated by N,N'-diisopropylcarbodiimide (DIC) to the

isonicotinic acid (mPSi-APTS-ISN), the characteristic frequency of the angular deformation of the NH bond emerges at 1550 cm^{-1} in the spectrum of mPSi-APTS-ISN meaning this molecule was covalently attached to APTS, as proposed in Figure 1.

Figure 6 (B) shows the UV-Vis spectra in the solid state of mPSi-APTS-ISN-Ruphen (red line) and mPSi-APTS-ISN (black line) along with the spectra of the cis-[RuCl(ISN)(dppb)(phen)](PF$_6$) (RuphenISN, green line) and cis-[RuCl$_2$(dppb)(phen)] (Ruphen, blue line) complexes. Knowing that the parent silica-based material mPSi presents no electronic transitions from 200 to 800 nm, all the absorptions observed in the UV-Vis spectra of mPSi-APTS-ISN and mPSI-APTS-ISN-Ruphen are ascribed to the species that decorate the microspheres. The spectra of the non-immobilized RuphenISN and Ruphen complexes show bands at high energies (up to 280 nm) assigned to the intraligand transitions of the ISN, phen and dppb moieties.[44,45] These absorptions are also observed in the spectra of mPSi-APTS-ISN and mPSI-APTS-ISN-Ruphen confirming the modification of the silica with these molecules as anticipated by NMR and IR data. At wavelengths higher than 280 nm, the spectrum of the non-immobilized precursor complex (Ruphen, blue line) shows one broad band with maximum at ca 470 nm ascribed[28] to metal-to-ligand charge-transfer (MLCT) transitions to the phen and dppb moieties. For the RuphenISN complex (green line), another broad band at ca 430 nm is observed being assigned to the MLCT transitions from the dπ
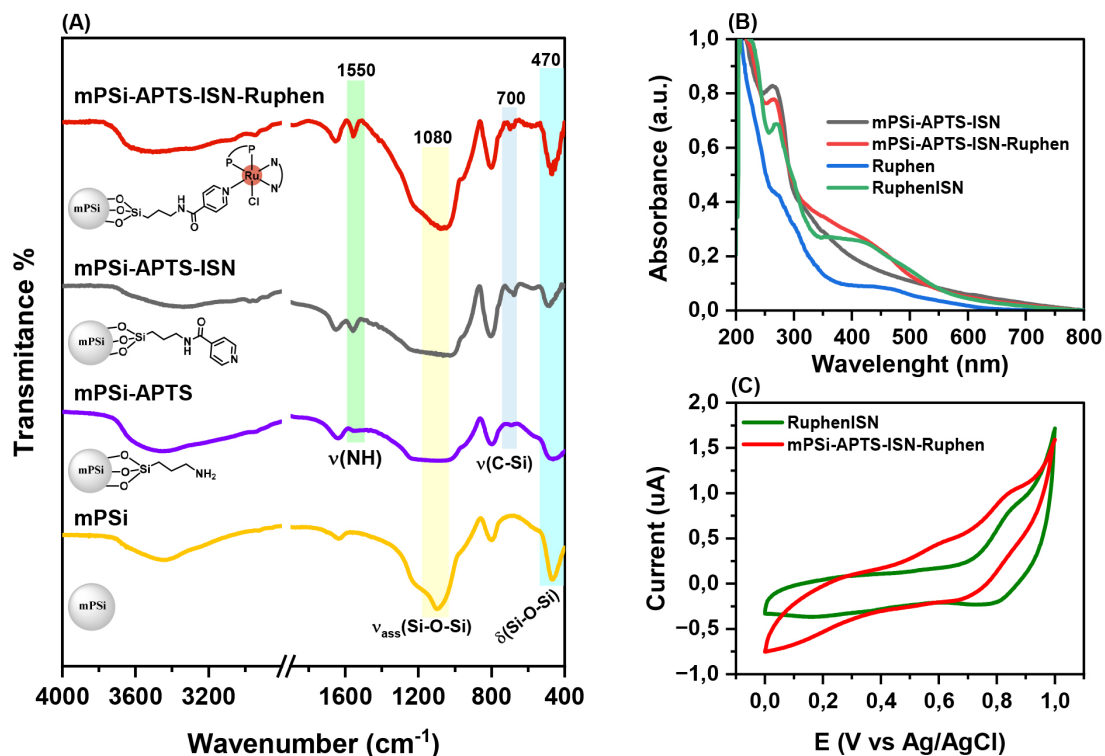

Figure 6. (A) FTIR spectra of mPSi, mPSi-APTS, mPSi-APTS-ISN, and mPSi-APTS-ISN-Ruphen; (B) UV-Vis spectra of RuphenISN, Ruphen, mPSi-APTS-ISN-Ruphen, and mPSi-APTS-ISN dispersed in KBr; (C) cyclic voltammograms in 0.1 mol L^{-1} solution of NaTFA (pH 3.5) at 100 mV s^{-1} of RuphenISN and mPSi-APTS-ISN-Ruphen dispersed in carbon paste

orbitals of Ru^{II} to ISN thus indicating the coordination of this species to the ruthenium metal center. The spectral similarity between the spectrum of the non-immobilized RuphenISN complex with that of the mPSI-APTS-ISN-Ruphen material (red line) indicates the ISN ligand previously attached to APTS was successfully coordinated to [RuCl(dppb)(phen)].

Cyclic voltammetry was also applied to characterize both the non-immobilized RuphenISN complex and the modified silica material. The cyclic voltammograms obtained for both samples, Figure 6 (C), show two waves centered at *ca.* 0.8 V *vs* Ag/AgCl ascribed to the Ru$^{III/II}$ redox pair. The positive potential shift in respect to the precursor complex (Ruphen, half-wave potential at 0.74 V Ag/AgCl in the same condition, data not shown), is consistent with the replacement of a π donor ligand (Cl$^-$) by a π acceptor species (ISN). Similar behavior has been reported for ruthenium complexes containing dppb and ligands of structures resembling that of ISN, like 4-methylpyrine and 4-aminopyridine in the coordination sphere.[15,46-48]

3.4. Thermogravimetric analysis

Thermogravimetric (TG) and differential thermal analysis (DTA) curves were obtained (Figure S3) to evaluate the thermal stability of the material. All the samples presented mass loss within the temperature range from 25 to 200 $^{\circ}$C associated with water and superficial silanol groups[49] wherein the non-modified microspheres showed the highest percentage (*ca* 7.5 %). This sample also showed events from 200 to 800 $^{\circ}$C related to the decomposition of the internal silanol groups whereas those on surface underwent condensation reaction producing siloxane (Si−O−Si), as seen in the infrared spectrum.[49] For mPSi-APTS and mPSi-APTS-ISN, the mass losses observed from 250 to 450 °C and from 450 to 650 °C were assigned[50-52] to the decomposition of the organic material localized on the surface and inside the microporous of the silica material,[53] respectively. For the sample containing the ruthenium complex, a more pronounced mass loss was observed (*ca* 15%) from 200 to 420 °C being an expected result if assuming the incorporation of the organic moieties added to the silica material (ISN, dppb and phen).

3.5. Leaching assays

As pointed out in the Introduction Section, a relevant concern on the use of catalysts attached to solid supports in heterogenous catalysis is the possible leaching into the liquid medium that would result in loss of catalytic activity and prevent recycling and reuse after the reaction. To evaluate whether the modifying procedure of the silica microspheres proposed in this work produced a material robust enough to keep the compound into the silica after being subjected to conditions typically applied in catalytic hydrogenation reactions of ketones, leaching assays were monitored by UV-Vis spectroscopy. The experiments were performed in basic solution (KOH in isopropyl alcohol) at 100 $^{\circ}$C and 2 atm H$_2$ pressure. Apart from the absorption of the isopropyl alcohol at high energy (below 300 nm) no meaningful absorption was seen (Figure S4) even after 24 h of stirring of the mPSI-APTS-ISN-Ruphen material in such medium.

4. Conclusions

This work presented a stepwise strategy to coordinate a ruthenium metal center to isonicotinic acid (ISN) previously attached to silica functionalized with 3-aminopropyltriethoxysilane (APTS). Such strategy was adopted aiming to produce a robust material in which the attached complex would undergo no leaching from the solid support thus allowing recycling and reuse if used for heterogeneous catalysis. At first, the silica-based material was functionalized with APTS giving mPSi-APTS. In the second step, the attachment of ISN to mPSi-APTS was achieved through an amide coupling mediated by *N,N'*-diisopropylcarbodiimide, producing mPSi-APTS-ISN. Finally, the coordination of the ISN ligand to *cis*-[RuCl$_2$(dppb)(phen)], where dppb = bis(diphenylphosphine)butane, phen = 1,10-phenanthroline, was performed by reacting this complex with mPSi-APTS-ISN and generating mPSi-APTS-ISN-Ruphen. Scanning electron microscopy indicated the prevalence of spherical particles of average size of 1.5 mm while N$_2$ adsorption/desorption isotherms showed H4 hysteresis loops consistent with micro (< 2 nm) and meso porous wherein the former dominates. The successive modifications steps resulted in a decrease of the surface area, pore diameter, and pore volume. For the mPSi-APTS-ISN-Ruphen sample, however, a meaningful increase of the pore diameter was observed being likely associated to a disruption of the outermost pores that led to a diameter increase. The observation of chemical shifts (170-120 ppm) in the solid NMR spectra consistent with *sp*^{2} carbons of ISN, dppb and phen moieties indicated the coordination of the ruthenium metal center to the ISN moiety previously attached to silica. This conclusion was reinforced by the similarity of the electrochemical and spectroscopic results obtained for mPSi-APTS-ISN-Ruphen with those acquired for the non-immobilized complex *cis*-[RuCl(ISN)(dppb)(phen)](PF$_6$), which was synthesized for the first time and fully characterized. The robustness of the mPSi-APTS-ISN-Ruphen material regarding the leaching of the ruthenium complex was evaluated in conditions typically applied in catalytic hydrogenation reactions of ketones and monitored by UV-Vis spectroscopy. After 24 h under stirring in basic alcoholic solution at 100 $^{\circ}$C and 2 atm H$_2$ pressure, the UV-Vis spectrum of the solution showed no absorption indicating the leaching of the complex into the solution. This results hints that the silica-based

material covalently modified with RuphenISN is robust enough to keep the compound into the silica ensuring its recycling and reuse thus offering a feasible strategy in line with the environmental sustainability.

Supplementary Information

Acknowledgments

Authorship Contribution

Ricardo D. Bernardo, Pedro M. Silva Filho, and Maria K. O. Abreu: methodology (syntheses and characterizations of the nanoparticles and the complexes), investigation, validation, data curation, writing-original draft. Dieric S. Abreu and Elisane Longhinotti: formal analysis, data curation, and editing. Izaura C. N. Diógenes: conceptualization, supervision, funding acquisition, project administration, writing-reviewing and editing.

References

1. Shakeri, E.; Blumel, J.; Creating Well-Defined monolayers of phosphine linkers incorporating ethoxysilyl groups on silica surfaces for superior immobilized catalysts. *Applied Surface Science* **2023**, *615*, 156380. [Crossref]

2. Silva Filho, P. M.; Andrade, A. L.; Lopes, J. B. A. C.; Pinheiro, A. A.; Vasconcelos, M. A.; Fonseca, S. G. C.; Lopes, L. G. F.; Sousa, E. H. S.; Teixeira, E. H.; Longhinotti, E.; The biofilm inhibition activity of a NO donor nanosilica with enhanced antibiotics action. *International Journal of Pharmaceutics* **2021**, *610*, 121220. [Crossref]

3. Costa, J. A. S.; Jesus, R. A.; Santos, D. O.; Neris, J. B.; Figueiredo, R. T.; Paranhos, C. M.; Synthesis, functionalization, and environmental application of silica-based mesoporous materials of the M41S and SBA-n families: A review. *Journal of Environmental Chemical Engineering* **2021**, *9*, 105259. [Crossref]

4. Erigoni, A.; Diaz, U.; Porous silica-based organic-inorganic hybrid catalysts: A review. *Catalysts* **2021**, *11*, 79. [Crossref]

5. Asal, M.; Özen, Ö.; Şahinler, M.; Baysal, H. T.; Polatoğlu, İ.; An overview of biomolecules, immobilization methods and support materials of biosensors. *Sensor Review* **2019**, *39*, 377. [Crossref]

6. Luan, Q.; Zhang, H.; Lei, Y.; Cai, Y.; Bao, Y.; Li, Y.; Tang, H.; Li, X.; Microporous regenerated cellulose-based macrogels for covalent immobilization of enzymes. *Cellulose* **2021**, *28*, 5735. [Crossref]

7. Liao, Y.; Cheng, Z.; Zuo, W.; Thomas, A.; Faul, C. F. J.; Nitrogen-rich conjugated microporous polymers: Facile synthesis, efficient gas storage, and heterogeneous catalysis. *ACS Applied Materials & Interfaces* **2017**, *9*, 38390. [Crossref]

8. Wang, J.; Jia, Z.; Metal nanoparticles/porous silicon microcavity enhanced surface plasmon resonance fluorescence for the detection of DNA. *Sensors* **2018**, *18*, 661. [Crossref]

9. Silva Filho, P. M.; Paz, I. A.; Nascimento, N. R. F.; Santos, C. F.; Araújo, V. R.; Aquino, C. P.; Ribeiro, T. S.; Vasconcelos, I. F.; Lopes, L. G. F.; Sousa, E. H. S.; *et al.*; Incorporation of nitroprusside on silica nanoparticles—A Strategy for safer use of this NO donor in therapy. *Molecular Pharmaceutics* **2019**, *16*, 2912. [Crossref]

10. Shinde, P. S.; Suryawanshi, P. S.; Patil, K. K.; Belekar, V. M.; Sankpal, S. A.; Delekar, S. D.; Jadhav, S. A.; A brief overview of recent progress in porous silica as catalyst supports. *Journal of Composites Science* **2021**, *5*, 75. [Crossref]

11. Paredi, P.; Pandey, M.; Tsunoji, N.; Prajapati, R.; Das, S.; Bandyopadhyay, M.; Mononuclear Cu-complex embedded ordered nano-porous silica based hybrid catalyst for oxidation of benzyl alcohol. *Molecular Catalysis* **2023**, *547*, 113357. [Crossref]

12. Yaacoub, L.; Dutta, I.; Wergh, B.; Chen, B. W. J.; Zhang, J.; Hamad, E. A.; Ang, E. P. L.; Pump, E.; Sedjerari, A. B.; Huang, K.-W.; Basset, J.-M.; Formic Acid Dehydrogenation via an Active Ruthenium Pincer Catalyst Immobilized on Tetra-Coordinated Aluminum Hydride Species Supported on Fibrous Silica Nanospheres. *ACS Catalysis* **2022**, *12*, 14408. [Crossref]

13. Martínez-Aguirre, M.; Serrando, E.; Ezquerro, C.; Lalinde, E.; Berenguer, J. R.; Garcia-Martínez, J.; Rodríguez, M. A.; Hybrid organometallo-silica catalysts for sustainable visible-light promoted olefin isomerization. *Catalysis Today* **2023**, *422*, 114213. [Crossref]

14. Kalsin, A. M.; Peganova, T. A.; Sinopalnikova, I. S.; Fedyanin, I. V.; Belkova, N. V.; Deydier, E.; Poli, R.; Mechanistic diversity in acetophenone transfer hydrogenation catalyzed by ruthenium iminophosphonamide complexes. *Dalton Transactions* **2020**, *49*, 1473. [Crossref]

15. Silveira, R. G. d.; Higuera-Padilla, A. R.; Cunha, B. N. d.; Neto, J. H. d. A.; Catão, A. J. L.; Colnago, L. A.; Castellano, E. E.; Batista, A. A.; Synthesis, structure determination and catalytic activity of a novel ruthenium(II) [RuCl(dppb)(44bipy)(4-pic)] PF6 Complex. *Journal of Brazilian Chemical Society* **2021**, *32*, 10. [Crossref]

16. Chaplin, A. B.; Dyson, P. J.; Influence of arene dissociation and phosphine coordination on the catalytic activity of RuCl(kappa(2)-triphos)(p-cymene) PF6. *Journal of Organometallic Chemistry* **2011**, *696*, 2485. [Crossref]

17. Araujo, M. P.; Figueiredo, A. T.; Bogado, A. L.; Von Poelhsitz, G.; Ellena, J.; Castellano, E. E.; Donnici, C. L.; Comasseto, J. V.; Batista, A. A.; Ruthenium phosphine/diimine complexes: Syntheses, characterization, reactivity with carbon monoxide, and catalytic hydrogenation of ketones. *Organometallics* **2005**, *24*, 6159. [Crossref]

18. Ji, J.; Shi, L.-M.; Wu, F.; Xin, Z.-F.; Jia, A.-Q.; Zhang, Q.-F.; Syntheses, structures, and immobilization of ruthenium(II) complexes with alkoxysilane groups functionalized N,N'-diamine and phosphine ligands. *Journal of Coordination Chemistry* **2020**, *73*, 1314. [Crossref]

19. Calmettes, S.; Albela, B.; Hamelin, O.; Ménage, S.; Miomandre, F.; Bonneviot, L.; Multistep anchoring of a catalytically active ruthenium complex in porous mesostructured silica. *New Journal of Chemistry* **2008**, *32*, 727.[Crossref]

20. He, H.; Li, W.; Xie, Z.; Jing, X.; Huang, Y.; Ruthenium complex immobilized on mesoporous silica as recyclable heterogeneous catalyst for visible light photocatalysis. *Chemical Research in Chinese Universities* **2014**, *30*, 310. [Crossref]

21. Carrillo, A. I.; Schmidt, L. C.; Marín, M. L.; Scaiano, J. C.; Mild synthesis of mesoporous silica supported ruthenium nanoparticles as heterogeneous catalysts in oxidative Wittig coupling reactions. *Catalysis Science & Technology* **2014**, *4*, 435. [Crossref]

22. Heba, M.; Stradomska, D.; Szymańska, K.; Jarzębski, A.; Ambroziak, K.; Masternak, M.; Kolanowska, A.; Pudło, W.; Kuźnik, N.; Engineering and performance of ruthenium complexes immobilized on mesoporous siliceous materials as racemization catalysts. *Catalysts* **2021**, *11*, 316. [Crossref]

23. Liang, Y.; Recent advanced development of metal-loaded mesoporous organosilicas as catalytic nanoreactors. *Nanoscale Advances* **2021**, *3*, 6827. [Crossref]

24. Sisodiya, S.; Lazar, A.; Shylesh, S.; Wang, L.; Thiel, W. R.; Singh, A. P.; Covalently anchored ruthenium–phosphine complex on mesoporous organosilica: Catalytic applications in hydrogenation reactions. *Catalysis Communications* **2012**, *25*, 22.[Crossref]

25. Al-Noaimi, M.; Awwadi, F. F.; Hammoudeh, A.; Tanash, M.; Mixed thioalkyl-azoimine (SNN')/α-diimine–ruthenium complexes: synthesis, characterization, DFT calculations, crystal structure and application as pre-catalysts for hydrogenation of acetophenone. *Transition Met Chem* **2019**, *44*, 355. [Crossref]

26. Canivet, J.; Karmazin-Brelot, L.; Süss-Fink, G.; Cationic arene ruthenium complexes containing chelating 1,10-phenanthroline ligands. *Journal of Organometallic Chemistry* **2005**, *690*, 3202. [Crossref]

27. Jung, C. W.; Garrou, P. E.; Hoffman, P. R.; Caulton, K. G.; Reexamination of the reactions of Ph$_2$P(CH$_2$)nPPh$_2$ (n = 1-4) with RuCl$_2$(PPh$_3$)$_3$. *Inorganic Chemistry* **1984**, *23*, 726. [Crossref]

28. Queiroz, S. L.; Batista, A. A.; Oliva, G.; do Pi. Gambardella, M. T.; Santos, R. H. A.; MacFarlane, K. S.; Rettig, S. J.; James, B. R.; The reactivity of five-coordinate Ru(II) (1,4-bis(diphenylphosphino)butane) complexes with the N-donor ligands: ammonia, pyridine, 4-substituted pyridines, 2,2'-bipyridine, bis(o-pyridyl)amine, 1,10-phenanthroline, 4,7-diphenylphenanthroline and ethylenediamine. *Inorganica Chimica Acta* **1998**, *267*, 209.[Crossref]

29. Smith, N. A.; Zhang, P.; Salassa, L.; Habtemariam, A.; Sadler, P. J.; Synthesis, characterisation and dynamic behavior of photoactive bipyridyl ruthenium(II)-nicotinamide complexes. *Inorganica Chimica Acta* **2017**, *454*, 240.[Crossref]

30. Braga, T. P.; Gomes, E. C. C.; Sousa, A. F. d.; Carreño, N. L. V.; Longhinotti, E.; Valentini, A.; Synthesis of hybrid mesoporous spheres using the chitosan as template. *Journal of Non-Crystalline Solids* **2009**, *355*, 860. [Crossref]

31. Silva, F. O. N.; Gomes, E. C. C.; Francisco, T. S.; Holanda, A. K. M.; Diogenes, I. C. N.; de Sousa, E. H. S.; Lopes, L. G. F.; Longhinotti, E.; NO donors cis-[Ru(bpy)$_2$(L)NO (3+) and Fe(CN)(4)(L)NO (-) complexes immobilized on modified mesoporous silica spheres. *Polyhedron* **2010**, *29*, 3349. [Crossref]

32. Vansant, E. F.; Voort, P. V. D.; Vrancken, K. C.; *Characterization and chemical modification of the silica surface*; Elsevier, 1995.

33. Sing, K. S. W.; Physisorption of nitrogen by porous materials. *Journal of Porous Materials* **1995**, *2*, 5. [Crossref]

34. Barrett, E. P.; Joyner, L. G.; Halenda, P. P.; The determination of pore volume and area distributions in porous substances. I. Computations from nitrogen isotherms. *Journal of the American Chemical Society* **1951**, *73*, 373. [Crossref]

35. Thommes, M.; Kaneko, K.; Neimark, A. V.; Olivier, J. P.; Rodriguez-Reinoso, F.; Rouquerol, J.; Sing, K. S. W.; Physisorption of gases, with special reference to the evaluation of surface area and pore size distribution (IUPAC Technical Report). *Pure and Applied Chemistry* **2015**, *87*, 1051. [Crossref]

36. Zdravkov, B.; Čermák, J.; Šefara, M.; Janků, J.; Pore classification in the characterization of porous materials: A perspective. *Open Chemistry* **2007**, *5*, 385. [Crossref]

37. Tan, Y. H.; Davis, J. A.; Fujikawa, K.; Ganesh, N. V.; Demchenko, A. V.; Stine, K. J.; Surface area and pore size characteristics of nanoporous gold subjected to thermal, mechanical, or surface modification studied using gas adsorption isotherms, cyclic voltammetry, thermogravimetric analysis, and scanning electron microscopy. *Journal of Materials Chemistry* **2012**, *22*, 6733. [Crossref]

38. Weber, D.; Sederman, A. J.; Mantle, M. D.; Mitchell, J.; Gladden, L. F.; Surface diffusion in porous catalysts. *Physical Chemistry Chemical Physics* **2010**, *12*, 2619. [Crossref]

39. Babonneau, F.; Baccile, N.; Laurent, G.; Maquet, J.; Azaïs, T.; Gervais, C.; Bonhomme, C.; Solid-state nuclear magnetic resonance: A valuable tool to explore organic-inorganic interfaces in silica-based hybrid materials. *Comptes Rendus Chimie* **2010**, *13*, 58. [Crossref]

40. Pazderski, L.; Pawlak, T.; Sitkowski, J.; Kozerski, L.; Szłyk, E.; 1H NMR assignment corrections and 1H, 13C, 15N NMR coordination shifts structural correlations in Fe(II), Ru(II) and Os(II) cationic complexes with 2,2'-bipyridine and 1,10-phenanthroline. *Magnetic Resonance in Chemistry* **2010**, *48*, 450. [Crossref]

41. Fabian, R. H.; Klassen, D. M.; Sonntag, R. W.; Synthesis and spectroscopic characterization of ruthenium and osmium complexes with sterically hindering ligands. 3. Tris complexes with methyl- and dimethyl-substituted 2,2'-bipyridine and 1,10-phenanthroline. *Inorganic Chemistry* **1980**, *19*, 1977. [Crossref]

42. Steel, P. J.; LaHousse, F.; Lerner, D.; Marzin, C.; New ruthenium(II) complexes with pyridylpyrazole ligands. Photosubstitution and proton, carbon-13, and ruthenium-99 NMR structural studies. *Inorganic Chemistry* **1983**, *22*, 1488. [Crossref]

43. Busca, G.; Resini, C.; Vibrational Spectroscopy for the Analysis of Geological and Inorganic Materials. In *Encyclopedia of Analytical Chemistry*.

44. Fantacci, S.; De Angelis, F.; Sgamellotti, A.; Re, N.; A TDDFT study of the ruthenium(II) polyazaaromatic complex [Ru(dppz) (phen)$_2$]$^{2+}$ in solution. *Chemical Physics Letters* **2004**, *396*, 43. [Crossref]

45. Park, H.-J.; Kim, W.; Choi, W.; Chung, Y. K.; Ruthenium(II) complexes incorporating the bidentate ligand containing an imidazolium moiety: synthesis, characterization, and electrochemical properties and their application in a visible-light induced hydrogen-evolving system. *New Journal of Chemistry* **2013**, *37*, 3174. [Crossref]

46. Frazão Barbosa, M. I.; Valle, E. M. A.; Queiroz, S. L.; Ellena, J.; Castellano, E. E.; Malta, V. R. S.; de Sousa, J. R.; Piro, O.; de Araujo, M. P.; Batista, A. A.; On the synthesis and structures of the complexes [RuCl(L)(dppb)(N–N)]PF$_6$ (L=CO, py or 4-NH$_2$py; dppb=1,4-bis(diphenylphosphino)butane; N–N=2,2'-bipyridine or 1,10-phenanthroline) and [(dppb)(CO)Cl$_2$-Ru-pz-RuCl$_2$(CO)(dppb)] (pz=pyrazine). *Polyhedron* **2010**, *29*, 2297. [Crossref]

47. Pinheiro, S. O.; de Sousa, J. R.; Santiago, M. O.; Carvalho, I. M. M.; Silva, A. L. R.; Batista, A. A.; Castellano, E. E.; Ellena, J.; Moreira, I. S.; Diogenes, I. C. N.; Synthesis, characterization and structure of ruthenium(II) phosphine complexes with N-heterocyclic thiolate ligands. *Inorganica Chimica Acta* **2006**, *359*, 391. [Crossref]

48. Valle, E. M. A.; Lima, B. A. V.; Ferreira, A. G.; do Nascimento, F. B.; Deflon, V. M.; Diogenes, I. C. N.; Abram, U.; Ellena, J.; Castellano, E. E.; Batista, A. A.; Driving forces in substitution reactions of octahedral complexes: The influence of the competitive effect. *Polyhedron* **2009**, *28*, 3473. [Crossref]

49. Iler, R. K.; *The chemistry of silica: Solubility, polymerization, colloid and surface properties and biochemistry of silica*; Wiley, 1979.

50. Mueller, R.; Kammler, H. K.; Wegner, K.; Pratsinis, S. E.; OH surface density of SiO$_2$ and TiO$_2$ by thermogravimetric analysis. *Langmuir* **2003**, *19*, 160. [Crossref]

51. Yan, X.; Zhang, L.; Zhang, Y.; Qiao, K.; Yan, Z.; Komarneni, S.; Amine-modified mesocellular silica foams for CO$_2$ capture. *Chemical Engineering Journal* **2011**, *168*, 918. [Crossref]

52. Denysenko, D.; Grzywa, M.; Jelic, J.; Reuter, K.; Volkmer, D.; Scorpionate-type coordination in MFU-4l metal–organic frameworks: small-molecule binding and activation upon the thermally activated formation of open metal sites. *Angewandte Chemie International Edition* **2014**, *53*, 5832. [Crossref]

53. Jaroniec, C. P.; Gilpin, R. K.; Jaroniec, M.; Adsorption and thermogravimetric studies of silica-based amide bonded phases. *The Journal of Physical Chemistry B* **1997**, *101*, 6861. [Crossref]